Review Article

Biomechanics of Transcatheter Aortic Valve Replacement Complications and Computational Predictive Modeling

Fateme Esmailie, PhD [a,1], Atefeh Razavi, PhD [a,1], Breandan Yeats, BS [a],
Sri Krishna Sivakumar, BTech [a], Huang Chen, PhD [a], Milad Samaee, PhD [a], Imran A. Shah, BS [a],
Alessandro Veneziani, PhD [b], Pradeep Yadav, MD [c], Vinod H. Thourani, MD [d],
Lakshmi Prasad Dasi, PhD [a,*]

[a] The Wallace H. Coulter Department of Biomedical Engineering, Georgia Institute of Technology/Emory University School of Medicine, Atlanta, Georgia, USA
[b] Department of Mathematics, Department of Computer Science, Emory University, Atlanta, Georgia, USA
[c] Department of Cardiology, Marcus Valve Center, Piedmont Heart Institute, Atlanta, Georgia, USA
[d] Department of Cardiovascular Surgery, Marcus Valve Center, Piedmont Heart Institute, Atlanta, Georgia, USA

ARTICLE INFO

ABSTRACT

Transcatheter aortic valve replacement (TAVR) is a rapidly growing field enabling replacement of diseased aortic valves without the need for open heart surgery. However, due to the nature of the procedure and nonremoval of the diseased tissue, there are rates of complications ranging from tissue rupture and coronary obstruction to paravalvular leak, valve thrombosis, and permanent pacemaker implantation. In recent years, computational modeling has shown a great deal of promise in its capabilities to understand the biomechanical implications of TAVR as well as help preoperatively predict risks inherent to device–patient-specific anatomy biomechanical interaction. This includes intricate replication of stent and leaflet designs and tested and validated simulated deployments with structural and fluid mechanical simulations. This review outlines current biomechanical understanding of device-related complications from TAVR and related predictive strategies using computational modeling. An outlook on future modeling strategies highlighting reduced order modeling which could significantly reduce the high time and cost that are required for computational prediction of TAVR outcomes is presented in this review paper. A summary of current commercial/in-development software is presented in the final section.

ABBREVIATIONS

3D, three-dimensional; AS, aortic stenosis; CAD, computer-aided design; CFD, computational fluid dynamics; CO, coronary obstruction; CT, computed tomography; FE, finite element; FSI, fluid-structure interaction; IGA, isogeometric analysis; LC, left coronary; LCAh, left coronary artery height; MOR, model order reduction; MS, membranous septum; NURBS, nonuniform rational B-splines; POD, proper orthogonal decomposition; PPI, permanent pacemaker implantation; PPM, patient-prosthetic mismatch; PVL, paravalvular leak; RC, right coronary; SAVR, surgical aortic valve replacement; SOVd, sinus of Valsalva diameter; SV, singular values; TAVR, transcatheter aortic valve replacement; THV, transcatheter heart valve; UQ, uncertainty quantification; ViV, valve-in-valve; VTC, virtual THV to coronary.

Introduction

Transcatheter aortic valve replacement (TAVR) is a minimally invasive procedure designed to replace stenotic aortic valves and is currently approved for patients at all levels of surgical risk. TAVR is rapidly increasing in its use due to randomized clinical trials showing equivalence to the more traditional highly invasive surgical aortic valve replacement (SAVR). Recent U.S. Food and Drug Administration approval of low surgical risk patients enables treatment of most aortic valve diseased patients, setting the stage for TAVR to become the standard of care. Recent clinical data comparing TAVR to SAVR in low-risk patients showed a decrease in rehospitalization and mortality after 1

* Address correspondence to: Lakshmi Prasad Dasi, PhD, Department of Biomedical Engineering, Georgia Institute of Technology, 387 Technology Circle | Office 232, Atlanta, Georgia, 30313-2412, USA
  E-mail address: lakshmi.dasi@gatech.edu (L.P. Dasi).
  [1] Co-first authors.

year with TAVR; however, these differences were not seen after 2 years, with a notably higher incidence of valve thrombosis in the TAVR arm.[1] Thrombosis is just one of many adverse outcomes associated with TAVR, with others including but not limited to aortic root rupture, permanent pacemaker implantation (PPI), coronary obstruction (CO), and paravalvular leak (PVL).[2-6] Every heart center's multidisciplinary heart team, composed of cardiologists, surgeons, imaging specialists, nurses, co-ordinators, etc., engages in rigorous planning and development of clinical strategy for each patient using their collective experience and documented guidelines. At high-volume centers, severe adverse outcomes occur at low rates but still do occur. Additionally, lower-volume centers and less experienced operators are associated with higher patient mortality.[7] There is clearly a need for a better understanding of the biomechanical basis of these complications followed up with a more robust prediction and optimization method for even more rigorous planning.

Structural and fluid computational modeling is growing in accuracy and ability to model a wide range of valvular diseased states and clinical procedures. Previous studies range from basic native valve mechanics,[8-10] finite element (FE) simulation of transcatheter heart valve (THV) deployment,[11-13] computational fluid dynamics (CFD) and fluid-structure interaction (FSI),[14-16] and use of highly intricate biological material models.[17,18] These studies have improved our insight into the biomechanics and hemodynamics of various diseased states and provided information on the optimal treatment procedures.

TAVR computational modeling is widely reported for both self-expandable and balloon-expandable THVs.[11,19,20] Structural computational modeling has the ability to provide stress fields which have given insight into mechanisms such as root rupture and PPI.[21,22] CFD and FSI studies give further insight into mechanisms of PVL and thrombosis.[23,24] As a clinician, it is extremely valuable to have knowledge of the outcomes of computational studies involving TAVR to have a greater understanding of its mechanisms from a biomechanics standpoint and to see the usefulness in modeling capabilities toward future discovery and guideline implementation. This is especially true in specific patient morphologies such as severe calcification, bicuspid aortic valve disease, a failed bioprosthesis, and low coronary ostia. It has been shown that a well-developed computational model can provide physicians with a tool to make accurate decisions on matters such as the optimum depth of implantation.[25] The goal of this review is to present the current knowledge on adverse clinical outcomes following TAVR from a biomechanics and hemodynamics modeling perspective, as well as to offer an outlook on the current trends and how the field may benefit from computational modeling in the future. This paper is organized with sections focused on adverse outcomes in the order of root rupture, PPI, CO, leaflet thrombosis, patient prosthesis mismatch, and PVL. After this, we provide an outlook on advanced computational models and software that can help with preoperative planning using predictive modeling approaches.

Aortic Root Rupture

Aortic root rupture is a very rare and possibly fatal event following TAVR that requires immediate surgical intervention. Clinical trials have shown occurrence to be <1% with a higher incidence in heavily calcified aortic valves, including bicuspid aortic valves, with incidence up to 4.5%.[26,27] The reported mortality rate due to root rupture is 48%.[28] The mechanism for aortic root rupture is thought to be caused by calcium protrusion into the native tissue as a result of being pushed radially by the transcatheter stent.[3,28,29] This is known to only occur in balloon-expandable THVs and when a balloon is expanded following a self-expandable THV deployment, due to the balloon forcing the native valve to conform to its cylindrical shape. Prevention strategies in patients who have severe levels of calcium include choosing a smaller than normal recommended THV size and underexpansion of the balloon-expandable THV by decreasing the filling volume of the balloon to reduce the radial displacement of the calcium into the native tissue.[3] However, underexpansion can have adverse effects on pressure gradient

and may cause PVL.[6,30,31] Another possibility to avoid annular rupture is to send patients with heavy calcification in the landing zone to surgical AVR. Better understanding and prediction methods are required to optimize heavily calcified patient outcomes pertaining to aortic root rupture.

To understand the mechanisms, very limited computational studies have been performed analyzing aortic root rupture. Wang et al.[21] analyzed a single patient who had aortic root rupture postprocedurally and found high stresses in the aortic sinus at the location of rupture. This is demonstrated in Figure 1; it indicates a high stress region from the calcium deposits predicted by retrospective simulation of the new-generation SAPIEN S3 balloon-expandable THV in a patient who had root rupture.

Initial analysis detecting areas of aortic root rupture seems promising in its accuracy. However, measuring precise levels of stress and associating them with aortic root rupture are challenging due to the unknown patient-specific material stiffness and thickness. Moreover, stiffness and thickness are highly variable among the patients, with the strongest predictor of stiffness being age.[32] Strain of the native tissue at physiological pressure can be calculated based on the diameter change across the cardiac cycle, and by using patient-specific physiological blood pressure, a general stiffness metric can be calculated.[33,34] However, this method cannot predict the stiffness change at strains experienced during TAVR, which are higher than those seen in systole, and cannot predict the failure point of the tissue. Precise tissue thickness is difficult to measure due to the artifact blooming of the blood volume and low contrast between the tissue and the surrounding environment. Collectively, hyperelastic tissue properties and vessel thicknesses cannot be obtained from the computed tomography (CT) images and require alternative predictive methods.

Permanent Pacemaker Implantation

Reported occurrence rates of PPI for balloon-expandable THVs and self-expandable THVs are 20.7% and 25.5%, respectively.[4] The conduction system, located just below the membranous septum (MS) (Figure 2), may be blocked from the interaction between the THV and the native tissue.[35]

Measuring the MS length gives information on how much distance separates the aortic valve annulus from the location of the His bundle. MS length varies among patients with aortic stenosis (AS). Patients with tricuspid AS have a longer MS length than those with bicuspid AS.[36] The risk of conduction abnormalities and PPI is higher when the MS length below which the His bundle emerges is shorter. It has been shown by Jilaihawi et al.[37] that the self-expandable valve implantation depth below the length of the MS leads to a low prevalence of conduction disturbances and PPI. Knowing the MS length can assist in optimizing the implant depth to lower the risk of conduction disturbance and PPI,[38] but may not completely eliminate PPI occurrence.

Computational modeling of the THV deployment can assist in risk assessment by providing information on the contact forces on the native tissue as well as allowing for more precise device optimization with respect to deployment depth and THV sizing. The percent of the tissue area below the MS in contact with the THV stent, and the maximum contact pressure in this region, have been linearly correlated to PPI occurrence in a cohort of 112 patients who received a self-expandable THV.[39] The precise mechanism of conduction disturbance following TAVR from a biomechanical perspective remains unclear. Precise thresholds of contact forces that are required to cause different degrees of conduction disturbance as well as the accuracy of other parameters measured in computational analysis remain unknown. Additionally, not all patients develop conduction disturbance directly following TAVR, suggesting multiple mechanisms may exist that have different time dependencies. Retrospective computational modeling has also not been performed for balloon-expandable THVs, where the balloon contact could also be playing a role in conduction disturbance. The location of the His bundle is also difficult to determine, where a high level of contrast in the right side of the heart is required to identify the inferior
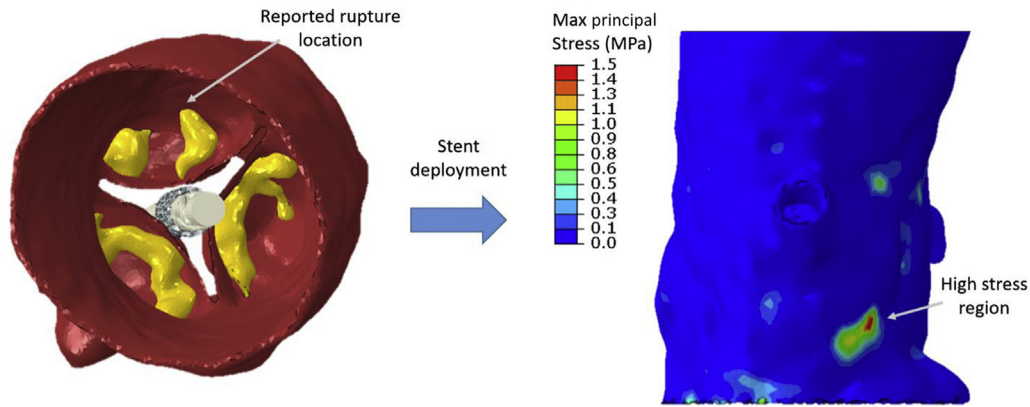
Figure 1. SAPIEN S3 transcatheter heart valve deployment in a patient who experienced aortic root rupture with detection of high stress in the region where the rupture occurred.

border of the MS, which only gives an area range of where the His bundle can be located, not the precise location. In conclusion, simple anatomical measurements can be taken to assist in deployment depth optimization to reduce PPI risk; however, conduction disturbance mechanisms across all THV types are still vague, where further computational analysis on larger patient cohorts can assist in bettering prediction algorithms.

Coronary Obstruction

CO is a procedural complication of TAVR that has been observed in 0.7% of all TAVR cases.[40] Anatomical predictors of CO include low coronary height, small sinus of Valsalva, female sex, and presence of previous surgical aortic bioprosthesis. According to Ribeiro et al.,[40] even though reported cases of post-TAVR symptomatic CO were rare,
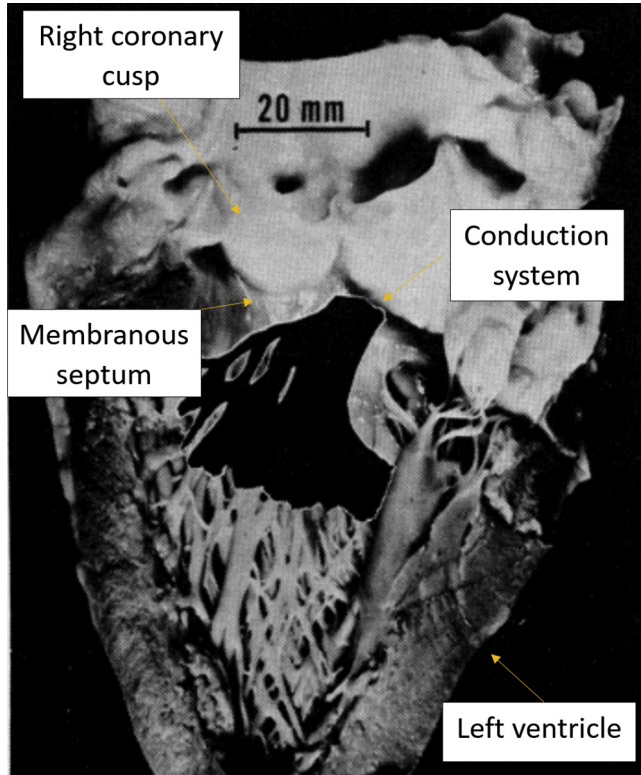

Figure 2. Conduction system location just below the membranous septum. Reprinted with permission from Massing GK, James TN. Anatomical configuration of the His bundle and bundle branches in the human heart. Circulation. 1976;53(4):609-621.[35] (https://www.ahajournals.org/doi/10.1161/01.CIR.53.4.609; The American Heart Association.)

life-threatening complications in balloon-expandable valve recipients, women, and patients with previous surgical bioprosthesis were more frequent. Acute and late mortality is reported to be high even after successful treatment in patients with a lower coronary ostium and shallow sinus of Valsalva.

Risk of CO is higher in patients with prior SAVR undergoing valve-in-valve (ViV) TAVR, with the incidence reported up to 6% compared to TAVI for native aortic valve disease.[41] Patients are often excluded from TAVR based on the guidelines of coronary height and sinus of Valsalva diameters derived from CT imaging, and hence, the number of patients at risk of CO with TAVR is probably underrepresented. In the event of CO, the failed aortic valve leaflets are displaced and obstruct one or both coronary arteries, resulting in immediate need for percutaneous coronary intervention or emergency coronary artery bypass grafting to resolve the occlusion. CO can present itself in a matter of a few hours or can be delayed[42] by weeks after the procedure. It is typically identified using coronary angiography after TAVR.[5]

Despite occurring in <1% of TAVR procedures, ostial CO is associated with high mortality rates of up to 50% within 30 days, leading to increased efforts to anticipate and prevent this life-threatening complication.[40,41] To estimate the risk of CO after TAVR, the left coronary artery height (LCAh) and sinus of Valsalva diameter (SOVd) are measured from preprocedural CT imaging. Thresholds of LCAh <12 mm and/or SOVd <30 mm were defined based on anatomical measurements of 44 out of 6688 patients who had CO after TAVR.[40] In the study by Ribeiro et al., 86% of the patients who had CO after TAVR had an LCAh of <12 mm, compared to 26.4% in the group with no CO ($p < 0.001$). The SOVd was <30 mm in 71.4% of the patients who had CO compared with 33% of the patients in the control group ($p < 0.001$). As many as one-third of the patients who underwent successful TAVR might have been excluded had these guidelines been applied previously. Patients who are deemed high surgical risk and present high risk of CO based on LCAh and SOVd after TAVR can still undergo TAVR safely with the help of techniques such as coronary protection or BASILICA.[43,44] However, current guidelines do not allow for quantitative estimation of the degree of obstruction, and therefore, the need for such protective measures is often uncertain.

To estimate CO risk for TAVR in failed bioprosthetic valves (ViV), a virtual THV to coronary (VTC) index has been defined using CT imaging.[45] The TAV device is replaced with an idealized cylinder that is drawn from the geometric center of the surgical prosthetic valve. The distance between the cylinder edge and coronary ostia is measured using CT imaging software. A low value of the VTC index suggests that there is a high risk for CO occurrence, with a VTC index <4 mm best predicting CO.[41] A more conservative threshold (VTC index <3 mm) was reported in an earlier publication.[46] However, similar to LCAh and SOVd, the VTC index does not account for the device interaction and anatomical risk factors such as small sinotubular junction diameters that could lead to sinus sequestration with ViV TAVR, potentially affecting the selectivity of the index.[41,45]
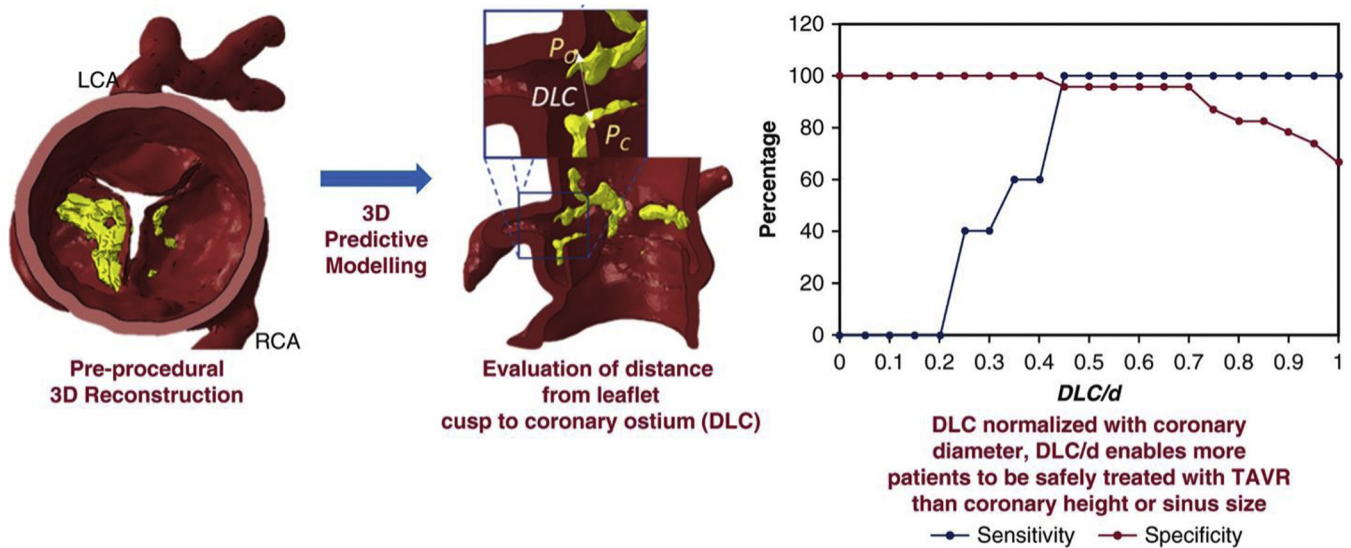
Figure 3. **Results of the simulation to obtain DLC and sensitivity/specificity curves for model.** Reprinted from Heitkemper et al.[48]

Computational Predictive Models

The role of computational modeling in predicting adverse outcomes such as annular rupture, conduction abnormalities, and PVL has been well demonstrated in the literature.[12,21,47] However, predictive computational models on CO have not been described until recently. Computational models account for certain anatomic factors such as calcific lesion size/location, leaflet length, sinus width at coronary ostium, etc. that are not considered in current clinical guidelines. Heitkemper et al.[48] have published a journal article on computational modeling for CO based on computational modeling of TAVR with FE methods (Figure 3). The objective of the computational model is to predict the closest distance between the coronary ostia and corresponding leaflet cusp after deployment of a TAV device. The model simulates the expansion of an idealized stent (cylinder) to the diameter of a TAV inside a patient-specific geometry that includes the calcification deposits on the leaflets. The closest distance between the native aortic valve leaflet and the tip of the coronary artery is then measured, and the ratio of this distance to the diameter of the corresponding coronary artery is considered a representative measure of the fraction of obstruction. Based on the sensitivity/specificity plots obtained from 28 cases retrospectively, a distance from leaflet cusp to coronary ostium (DLC) normalized with coronary artery diameter (DLC/d) parameter value of 0.7 was determined to be the cutoff for risk of CO. The (three-dimensional [3D]) computational model was 38% more effective (based on sensitivity and specificity analyses) at predicting CO than coronary artery height and 58% more effective than SOVd.

In another preliminary computational study by Sivakumar et al. (Figure 4),[49] preprocedural CT images of 17 patients undergoing ViV TAVR were collected from Piedmont Heart Institute, Atlanta, GA. Patient-specific geometries of the aortic root, bioprosthetic valve stent, and leaflets were reconstructed using segmentation. Computational TAVR modeling was simulated with both self-expandable Medtronic Evolut and balloon-expandable Edwards SAPIEN transcatheter aortic valves to compare the risk of CO between the 2 valve types. Additionally, virtual THV to coronary (VTC) distance was obtained for all cases for comparison. The mean left coronary (LC) and right coronary (RC) heights were 6.9 ± 3.05 mm and 9.17 ± 4.23 mm, respectively. The mean VTC LCA was 5.02 ± 2.39 mm and VTC RCA was 3.48 ± 1.58 mm. The mean DLC/d ratio for SAPIEN ViV (n = 12) was 0.61 ± 0.53 and 0.88 ± 0.53 for the LC and RC, respectively. The DLC/d for Evolut ViV (n = 10) was 0.77 ± 0.39 and 1.2 ± 0.63 for the LC and RC, respectively. In this study, the VTC cutoff of 4 mm overpredicted CO in 23.5% of cases and underpredicted the risk of CO in 35.3% of cases compared to DLC/d. A larger

cohort of ViV TAVR cases may be necessary to compare the accuracy of the 2 models.

Leaflet Thrombosis

The reported incidence rate for leaflet thrombosis in TAVR patients ranges from 4% to 40% in different studies.[2,50-57] However, most of the patients were asymptomatic or subclinical,[50,58] with less than 3% of the overall patients[59-62] showing symptoms such as dyspnea or heart failure. Most of the subclinical valve thromboses in TAVR are detected by postprocedural multidetector CT scans or tomography angiography,[63-65] which appears as a thin layer of thrombus on the aortic side of the prosthetic leaflet. This type of thrombosis is usually called hypoattenuating aortic leaflet thickening and is often associated with reduced leaflet motion and increased pressure gradient.[2,66,67] Valve thrombosis is usually treatable by anticoagulant or antiplatelet therapies.[60,61,68-71] Studies have identified risk factors associated with leaflet thrombosis, including male sex,[2] bicuspid valve,[68] moderate-to-severe PVL,[55,72] low-flow, low-gradient AS,[63] patient-prosthesis mismatch,[60,63,73] large Valsalva/TAVR prostheses,[2,72] absence of prescribed anticoagulation,[2,56,72] damage to leaflets during TAVR,[59] self-expandable intra-annular valve,[54,63] and ViV procedures.[59,68] Despite its prevalence, asymptomatic or subclinical leaflet thrombosis seems not to change the medium-term outcome, as indicated by multiple studies.[2,55,72,74] Other studies have suggested that subclinical leaflet thrombosis is more likely associated with stroke, transient ischemic attacks, and valve degeneration.[50,74] Due to the lack of long-term data, it is not clear whether it will affect the outcome of TAVR in the long run. Leaflet thrombosis has remained a great concern for the success of TAVR.

Thrombosis on bioprosthetic valves has also been observed in SAVR,[75,76] but with a lower incidence rate ($<4\%$[50]) than the rate for the TAVR thrombosis, suggesting that the TAVR thrombosis is primarily associated with its unique design and implantation method. Since the native leaflets are not removed during TAVR, a small region between the prosthetic and the native leaflets called the neosinus forms after the procedure. It was hypothesized that the flow stasis in this neosinus was the primary cause for thrombosis.[59] Vahidkhah et al.[77] used the one-way FSI model to show that the blood residence time was significantly longer for leaflets of a TAV than that for those with SAV. Also, they indicated that a supra-annular valve reduced flow stasis in TAVs.[78] In vitro experiments performed by Midha et al.[79] supported this theory. They found that when a supra-annular valve was deployed in the intra-annular position, it resulted in a sevenfold increase in the stagnation region. In vitro experiments also have shown that the neosinus washout time for a
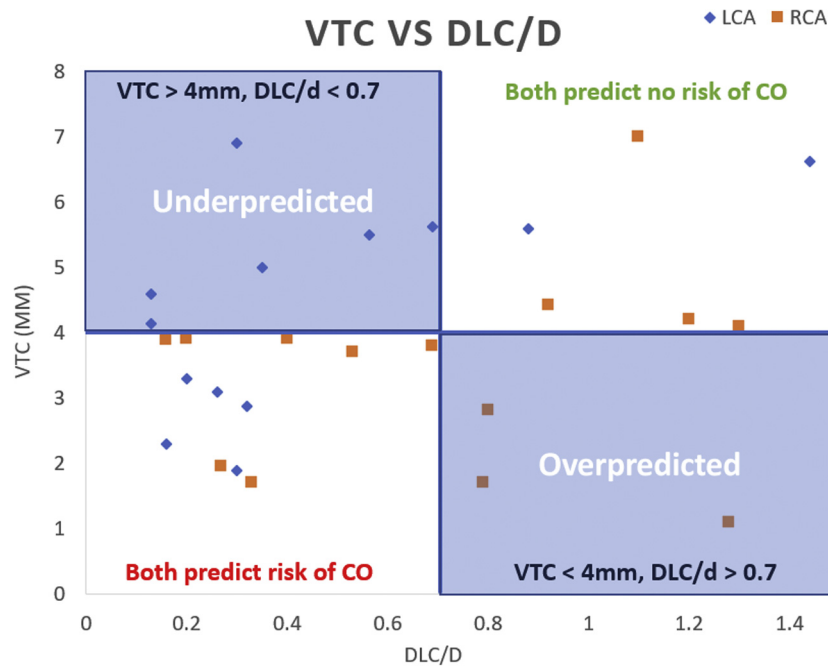
Figure 4. Comparison of risk of CO from computational modeling (DLC/d) with CT-based risk assessment (VTC) in 17 cases of ViV TAVR.
Abbreviations: CO, coronary obstruction; CT, computed tomography; TAVR, transcatheter aortic valve replacement; ViV, valve-in-valve; VTC, valve-to-coronary.

supra-annularly deployed valve was significantly lower than that for the same valve deployed intra-annularly. Those results were consistent with clinical observations that the intra-annular valves are more prone to thrombosis.[54,63] Based on this theory, a series of experimental and computational research has been carried out to study the risk factors and to find ways to minimize the thrombosis risk. The reported results on investigating the impact of underexpansion on the possibility of thrombosis after TAVR do not agree;[80,81] thus, further analysis of the impact of underexpansion is a necessity.

In a study by Madukauwa-David et al.,[82] it was shown that the coronary flow increased the neosinus washout, leaving the noncoronary leaflet more prone to thrombosis. A CFD study by Plitman Mayo et al.[83] was performed to estimate post-TAVR thrombosis potential in ViV cases and demonstrated that the intra-annularly deployed Sapien valves had a higher risk of thrombosis. Advanced predictive patient-specific modeling using sophisticated software was developed to reduce the risk of thrombosis in clinical practices. Wei et al.[84] provided a workflow to assess the risk of post-TAVR thrombosis. Bianchi et al. developed a patient-specific model of TAVR and post-TAVR CFD for patients with self- or balloon-expandable valves.[12,85] Gryzbon et al.[24] have shown computationally that the patient-specific anatomical and hemodynamic characteristics impacted the volume of thrombosis. They reported that the percentage of stasis volume is a linear function of thrombus volume.[24] Hatoum et al. developed a semi-empirical, mathematical dimensionless parameter called normalized circulation (a function of patient-specific anatomical and hemodynamic characteristics) that can be applied to predict the post-TAVR thrombus formation.[86,87]

Patient-Prosthesis Mismatch

Patient-prosthesis mismatch (PPM) occurs when the effective orifice area (EOA) of an implanted prosthetic aortic valve is much smaller than the native aortic annulus size.[88–91] In PPM, the prosthetic valve is enforced to have a high transprosthetic gradient to maintain sufficient stroke volume.[89,92] Severe cases of PPM (indexed EOA <0.65 cm^2/m^2, based on observational clinical studies) were thought to have an impact on increased risk of structural valve degeneration and overall mortality.[89,93] Several studies reported that PPM prevalence is lower following TAVR vs. SAVR.[94–97] Comparing the 2 types of TAVs, self expandable (SE) valves show lower PPM (larger EOA) than balloon expandable valves; Okuno

et al.[98] reported that PPM mainly differed in patients with larger body surface area, i.e., body surface area >1.83 m^2 comparing SE and balloon expandable valves. Abbas[99] explained that this difference is because of the discrepancy between echocardiography and invasive gradients due to the pressure recovery concept and limitation of the Bernoulli equation.[100] They added that echocardiography overestimates the aortic jet velocity and consequently peak gradient which leads to low EOA and severe PPM.[99,100] SE valves might also be associated with a higher PVL.[101–103]

In a meta-analysis study by Dayan et al.,[96] PPM predictors were reported as female sex, hypertension, older age, diabetes, and renal failure. They also reported lower mortality associated with PPM in patients with a higher body mass index. The prediction/prevention of PPM is of utmost importance since the only operative intervention after PPM incidence is repeating the surgery (or ViV TAVR procedure).

Paravalvular Leak

PVL is a leak due to the gap between the implanted valve and surrounding tissue structure. Despite enhancements in TAVR techniques, PVL is still a common postprocedural complication with variable reported incidence rates. This variability may be related to the varying imaging modalities used in different centers, evaluation timing, the grading system, and variability in prosthesis type.[104] According to Valve Academic Research Consortium-2,[105,106] PVLs are graded as no leaks, mild, moderate, and severe. More supporting evidence is required to validate these criteria and to develop robust quantitative methods for PVL localization, quantification, and severity assessment that cannot be achieved from the imaging modalities alone.[107] Computational modeling of TAVR has enhanced our understanding of PVL from both structural and hemodynamics standpoints. Using finite element analysis (FEA), CFD, and FSI analyses, PVL can be assessed under various scenarios including stent shapes, stent designs, stent orientation, valve positioning, and valve sizing. In computational modeling of TAVR, PVL is determined as the gap between the stent and native tissue or skirt in FEA and the PVL jet flow is calculated at the gap region in CFD and FSI analyses. Figure 5 is a demonstration of TAVR deployment results using FEA in a patient with a balloon-expandable valve validated by post-CT clinical images highlighting the gap region. CFD hemodynamic analysis detected PVL at a native commissure.[108]
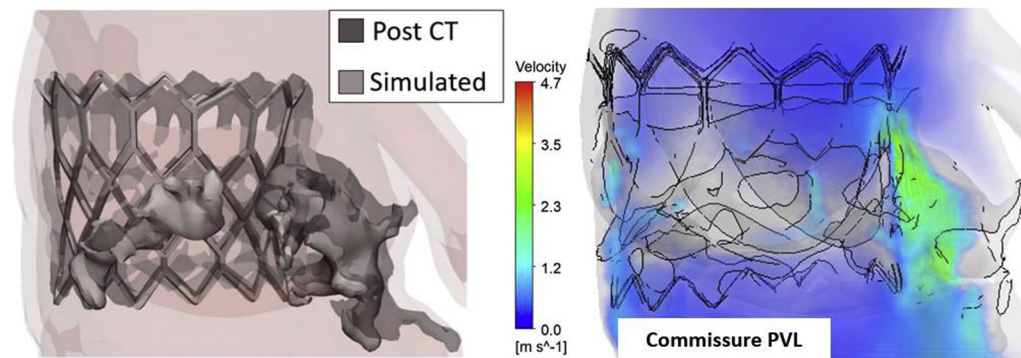
Figure 5. **FEA simulated deployment of a balloon-expandable THV in a good agreement with the postoperation CT stent geometry (left).** CFD hemodynamics analysis enabled PVL detection and quantification at a native commissure point due to incomplete sealing of the device. Reprinted by permission from Springer Nature, *Current Cardiology Reports*: Yeats, B.B., Yadav, P.K., Dasi, L.P. et al. Treatment of Bicuspid Aortic Valve Stenosis with TAVR: Filling Knowledge Gaps Towards Reducing Complications. Curr Cardiol Rep. 2022; 33–41, © 2022.[108]
Abbreviations: CFD, computational fluid dynamics; CT, computed tomography; FEA, finite element analysis; PVL, paravalvular leak; THV, transcatheter heart valve.

The patient-specific FEA modeling approach employed by most of these studies includes the following: 1) generating the computer-aided design (CAD) model of the stent frame, with or without including the prosthetic leaflets and skirt, from the micro CT data or standalone design, 2) reconstructing 3D geometry of the aortic root, native leaflets, and calcium deposits, 3) assigning material properties to the reconstructed parts, 4) crimping the stent, and 5) stent deployment or release by volume or pressure inflation of the balloon (for balloon-expandable stents) and radial expansion of the stent (for self-expandable stents). There is an intermediate step of prepressurizing the root due to the blood diastolic pressure that sometimes is missing from the TAVR computational studies due to the simulation complexities.[12,47,85,109]

Nappi et al.[109] used FEA to simulate SAPIEN and CoreValve deployment in 2 patients who had device failure and compared the FEA findings with the results from 2 patients with no postprocedural complication. They indicated that the CoreValve in the rehospitalized patient led to elliptical deformation that was greatest distally where a large amount of calcium was persisting. The values of the paravalvular and contact area were reported to be larger in rehospitalized patients for both valve types. In a combined FEA-CFD analysis by Mao et al.,[47] a CoreValve deployment was modeled with 3 orientations, 3 deployment heights, 2 skirt shapes, and 3 stent thicknesses. Their results showed that the PVL can differ up to 40% between the orientated models due to the scallop shape of the stent. They also reported a 70% change in the leaking volume between different deployment heights and found that the lower deployment may help reduce PVL. Bianchi et al.[12] performed FEA-FSI analyses in SAPIEN and CoreValve cases for 2 different positions as well as 2 valve sizes. The aortic and midway valve positions were used for the SAPIEN, and the aortic, midway, and ventricular positions were used for the CoreValve. The valve sizing was based on nominal and overexpansion of the stents. Their FEA findings showed that the SAPIEN with nominal expansion showed a higher potential for PVL having the lower contact area as well as the larger amounts of calcium than the other cases. FSI analysis also showed that SAPIEN had the largest PVL compared to the other cases. While both aortic and ventricular positioning resulted in an increase in PVL for both SAPIEN models, aortic positioning for the CoreValve resulted in PVL reduction. Luraghi et al.[16] studied 2 cases with clinical prognosis of mild and moderate PVL using FEA-FSI analyses. They designed a CAD model similar to the CoreValve, including the stent frame, bioprosthetic leaflets, and the skirt, and compared the results with the postprocedural CT data. They reported a good agreement between the computational data and Doppler measurements for the maximum velocity values at peak systole. Calculating velocity contour maps in several cross-sectional planes along the length of the aorta, they reported 1 minor PVLs for one case and one major PVL for the other case with the regurgitant volumes of 26.88 ml and 43.73 ml. In another study by

Luraghi et al.,[110] they examined the effect of calcification patterns on the TAV performance. They created an averaged aortic geometry from 1 patient-specific reconstructed models and generated "coaptation pattern or arch shaped" and "radial or circular pattern" of the calcium deposits on the leaflets. They showed that the radial pattern had a moderate PVL (25-26 mL) and coaptation pattern had a mild PVL (35-40 mL) according to Valve Academic Research Consortium-2.[105] Ghosh et al.[85] examined aortic, midway, and ventricular valve positioning similar to Bianchi et al.,[12] for an Evolut R valve. Additionally, they included the beating of the heart to analyze the valve anchorage. They reported PVL degrees of 34.59 ml and 41.61 ml for the midway and ventricular positioning, respectively. Considering PVL and other structural and hemodynamics factors, e.g., geometric orifice area, von Mises stresses, and thrombogenic potential, they concluded that anterior fibrous trigon ventricular positioning resulted in the optimal valve performance in that particular patient anatomy.

In summary, *in-vitro* and *in-silico* biomechanical studies provide detailed information on the anatomical features as well as their changes due to the device deployment, to detect the PVL site and to evaluate functional characteristics including biomechanical stress concentration and PVL severity. The methods developed, once validated on a large cohort, can be used to predict PVL and its association with other postprocedural complications and to assist in clinical, procedural, and surgical decision-making.

Outlook on Predictive Computational Models and Model-Order-Reduction Techniques

Computational models substantiate the third paradigm of investigation, the in silico one, after the traditional *in-vitro* and *in-vivo* models (see e.g. the study by Formaggia et al. and Auricchio et al.[111,112]). New techniques in computational mechanics, together with new computational infrastructures and imaging/data retrieval devices for patient-specific modeling, give new perspectives on the role of modeling from the initial proof-of-concept stage to the support of clinical trials (computer-aided clinical trials or *in-silico* clinical trials; see e.g. the study by Pappalardo et al.[113]), the design of therapy optimization,[114] and the assessment of sensitivity and impact of uncertain knowledge on the final result uncertainty quantification (UQ).[115-117] The need for fast and reliable numerical results pinpointed above motivated new computational techniques and modeling paradigms. Also, the modeling approaches introduced so far are not directly linked to clinical outcomes.

Traditional numerical techniques for solving the partial differential equation underlying mechanical models rely mainly on introducing a representation of the approximate solution as a linear combination of functions involving a finite number of coefficients. For instance, we can approximate the displacement of a structure under static conditions by a linear combination in the form

$$u(x, y, z) = \sum_{i=1}^{N} u_i \phi_i(x, y, z) \qquad (1)$$

where the coefficient u_i is computed by solving an algebraic system, while the basis function $\phi_i(x, y, z)$ can be selected in different ways. For instance, in the FE method, after a reticulation of the region of interest, these functions are piecewise polynomials on the mesh elements. Piecewise polynomials are easy to define, differentiate, and integrate. The basis functions are also generally nonzero only on a small number or patch of elements, leading to the solution of linear (or linearized) systems with a small number of nonzero entries, which implies a critical save of computational and storage resources. However, piecewise polynomials are a "general purpose" basis function set that can be virtually used for any differential problem. Consequently, in Eq (1), all the information about the problem to solve is in the coefficient u_i. The number N of coefficients required to have accurate solutions can be, therefore, quite large.

In CAD, the mathematical representation of components of a mechanical part, such as a prosthesis, is not generally done by generic piecewise polynomials like in FEs for their low regularity. In CAD, one of the main ingredients for the mathematical representation of objects is given by splines, particularly nonuniform rational B-splines (NURBS). These curves guarantee an excellent trade-off between regularity and ease of representation, causing them to be extremely popular in computer graphics and CAD. Isogeometric analysis (IGA) is a numerical technique introduced by Hughes et al.,[118] where NURBS are used to represent not only the domain of interest but also the solution of Eq (1) of the associated differential problem: the basis function ϕ_i is represented by NURBS. This approach automatically eliminates all the geometrical errors of the FE representation of the domain, with a significant computational advantage. In particular, IGA has been extensively used in the patient-specific computational modeling of aortic valve closure and TAVR deployment.[119,120] For instance, Morganti et al.[119] compared IGA with FEs for simulating aortic valve closure in a single patient and found that IGA resulted in valve coaptation profiles that resembled natural physiological conditions at a significantly reduced number of mesh nodes compared to typical FE analysis, thus leading to significantly reduced computational costs. Wu et al.[120] employed IGA in a computational FSI framework to form a technique known as immersogeometric analysis to analyze the radial outward force and friction force during TAVR deployment. Here, IGA was used to fully capture the complex geometry and discretize both the fluid and structural domains involved in the FSI problem, thus avoiding the difficulties seen at the fluid-solid interface with typical FE meshes.

IGA is an example of customization of Eq (1) to specific problems where using a more regular basis can introduce significant computational advantages. Other specific customizations based on a data-driven paradigm may be considered as well. These approaches belong to the general idea of "model order reduction" (MOR), where the number N degrees of freedom can be drastically reduced to make real-time computation a realistic target. Classical approaches of MOR rely on the sequence of 2 stages, off-line and online. The general purpose is to perform the heavy computations during the off-line, promptly leveraged in the online phase with a rapid solution. In short, we resort to a highly customized basis function set $\phi_i(x, y, z)$ obtained during the off-line phase, which contains much information about the problem to solve. In this way, the number N in Eq (1) significantly reduces to an order of hundreds or less. To exemplify the methodology (see, e.g. the study by Hesthaven et al. and Quarteroni et al.[121,122]), let us assume to work on a parametrized problem, such as a linearly elastic material parametrized by the Young modulus or the applied boundary conditions. After a traditional discretization (e.g., by FEs), several solutions can be computed in the off-line stage for different values of the parameters. These solutions (snapshots) form a database or library.

The selection of the values of the parameters to use for the snapshots can follow from a uniform sampling of the parameters' space or more sophisticated strategies. In fact, it may follow more rigorous criteria

(certified reduced basis method) such that the snapshots maximize the representativity of all the possible physical solutions in the parameter space. This "certified" approach requires certified estimates of the representativity of each snapshot in the parameter space that are not always available in practice. For this reason, we stick to the uniform sampling approach.

In the online stage, we rapidly compute the solution for generic values of the parameters by using the snapshot database. For linear problems featuring a linear dependence of the solution on the parameters, the superposition of effects promptly reconstructs the solution by a linear combination of snapshots. However, generally, the dependence of the solution on the parameters is not linear, and the superposition of effects cannot be advocated. Yet, we look for a solution in the space spanned by the snapshots. The coefficients of this linear combination can be obtained by projecting the full-order problem (e.g., the FE one) to the space spanned by the snapshots. This approach, in general, can still be ineffective, as the number of snapshots to adequately cover the parameter space can be pretty large. On the other hand, the level of information carried by the snapshots features a high redundancy, as each snapshot is solving the same problem, just with a different value of the parameters. To filter out this redundancy, we resort to a fundamental tool of linear algebra called singular value decomposition. This technique allows for identifying the principal components of the database in terms of singular values (SV) of the snapshot matrix (possibly reset by subtracting the snapshot average). In general, we order the SV in decreasing order. Rapid decay of the SV indicates a high level of redundancy. The model reduction is then attained by taking only the SV beyond a desired threshold. These indicate the relevant parts of the snapshot library, and the associated left eigenvectors form the basis function ϕ_i to represent the reduced-order model solution. The original problem is then projected on the space spanned by these eigenvectors. A fast decay of the SV implies a small number N to just hundreds of coefficients (vs. the thousands or more of the full-order model), with an evident computational advantage.

This approach goes under the name of proper orthogonal decomposition (POD), and it is one of the most popular MOR methods. Table 1 and Figure 6 demonstrate the implementation of POD for rapidly simulating the structural deformation of a Medtronic Corevalve.

A significant decrease in computational costs is seen after implementing the model reduction (Table 1), all while retaining the accuracy seen in the full order model solution (Figure 6). For nonlinear problems, the projection on the span of the eigenvectors requires special techniques that go under the name of the empirical interpolation method.[121] Efficient open-source libraries performing MOR with POD and certified reduced basis fluid and structural mechanics problems can be found at https://www.rbnicsproject.org/ and in the study by Demo et al.[123]

When computational models support clinical activity, the certification of the quality of the results becomes a critical step and, more precisely, the UQ (i.e., the assessment of the dependence and robustness) of the numerical results on the several uncertainties of the data becomes a critical step. UQ methods require probing of the computational model under several different conditions dictated by the stochastic distribution of the noise of the data, and it is therefore generally costly. MOR may play a fundamental role also in this respect.

Data-driven techniques based on machine learning (ML) complete the picture of new-generation quantitative methodologies, in particular

Table 1

Computational details for the FEM and ROM simulations

Mesh size	Number of snapshots computed	FE degrees of freedom	Number of reduced basis	Computational time (S)		
				FE simulation	ROM off-line	ROM online
257,671	105	227,511	13	102	2565	2.13

Notes. The reduced-order model (ROM) simulation is significantly faster than the finite element (FOM) simulation.
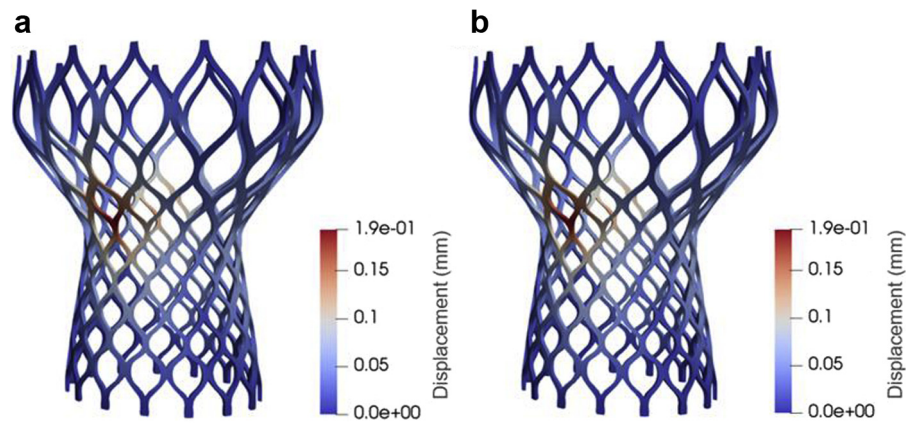FE, finite element.

Figure 6. Comparison of the displacement field for the reduced order model (ROM) solution (a) and the finite element model (FEM) solution (b).

when a well-established mathematical and numerical modeling is missing. For instance, Liu et al.[124] developed an ML model trained on FE simulations, capable of estimating constitutive parameters of the aortic wall within a significantly reduced computational time, i.e., a matter of seconds. In combination with the MOR mentioned above, such ML methods can rapidly provide material properties from patient-specific geometries that are necessary for the off-line phase of the MOR, thus resulting in a hybrid approach that is dramatically more accurate than standard MOR methods. In essence, this hybrid, data-driven ML-MOR approach provides a paradigm of predictive computational models in a real-time fashion and on local computational resources for clinical problems, including TAVR deployment.

Summary of Current Commercial and In-Development Available Computational Models

We summarized computational methods of TAVR complications and their pros and cons in the previous sections. Computational modeling of TAVR biomechanics and hemodynamics is mostly in the development stage, and it can be excelled by the technological innovations such as using future quantum computers and artificial intelligence algorithms. Some of the available pieces of computational software that are capable of simulating TAVR biomechanics and hemodynamics are listed below:

1. FEops provides a wide range of patient-specific planning simulations for TAVR and left atrial occlusion.[125] They are also developing their planning platform of transcatheter mitral valve replacement, transcatheter tricuspid valve replacement, and transcatheter pulmonary valve replacement. El Faquir et al.[25] showed that FEops HEARTguide impacted physicians' decision about the depth of implantation in TAVR with the self-expanding Evolute R valve, and they used FEops to find the optimum implantation depth. The focus of this software is on the structural valve simulations lacking hemodynamic considerations.
2. FlowVision (Capvidia NV, Leuven, Belgium) and Abaqus (Simulia, Dassault Syste`mes, Providence, RI, USA) coupling also allows for pre- and post-TAVR biomechanics and hemodynamics analyses. The advanced cut-cell method used in FlowVision employs complex polyhedron cells at the fluid-solid interface that are used to cut the Cartesian fluid domain, allowing the fluid cells conform based on the motion of the solid domain. Maintained precise features of the complex geometries without the need for a heavily refined mesh compared to the nonbody conforming techniques make the cut-cell method suitable for patient-specific valve assessments. Using these software packages, Kandail et al.[126] studied the impact of CoreValve implantation depth on aortic and coronary hemodynamics. Bianchi et al.[12] and Ghosh et al.[85] assessed leaflet kinematics, PVL, and thrombogenic potential after TAVR in a patient-specific manner. Emendi et al.[14] performed this coupling analysis to replicate hemodynamics in bicuspid AV patients which was validated against four-dimensional–flow magnetic resonance imaging measurements.
3. LS-DYNA (Livermore Software Technology Corporation, Livermore, CA) has been used in FEA-FSI analyses of the native and bioprosthetic valve computational modeling. Kivi et al.,[127] Marwan et al.,[128] and Cai et al.[129] simulated FSI in the idealized geometries of the aortic valve. Luraghi et al.[110] presented an FSI analysis in a patient-specific root. However, native leaflets and calcium patterns were not patient-specific. Fluid and solid domain discretization uses the arbitrary Lagrangian-Eulerian and nonbody conforming immersed boundary methods.
4. SimVascular is an open-source blood flow modeling and simulation tool.[130] This software provides a pipeline from extracting 3D geometric models from medical images to meshing and flow simulation. SimVascular has some FSI capabilities, and it includes physiologic boundary conditions and FE Navier-Stokes solvers.[131]
5. CRIMSON is open-source software that is capable of performing 3D hemodynamic simulations.[132] The FE method and reduced order computational methods are applied in developing this software. Vascular structure segmentation and construction of analytic arterial and venous models followed by a mesh generation algorithm are designed in the CRIMSON pipeline. After the FE mesh generation and applying boundary conditions, this software is able to solve Navier-Stokes equations for the blood flow. It also has some FSI features and can handle postprocessing and visualization tasks. CRIMSON has not been commercialized yet.[132] Also, it is not clearly stated if this software is capable of handling hemodynamic simulations with prosthetic valves or not.

There are other software available commercially that are predicting various cardiac adverse events, but these software are out of scope of this review paper, including Certara[133] (predicts the cardiotoxicity risk), openCARP[134] (a cardiac electrophysiology simulator), and CVSim[135] (an open-source cardiovascular system lumped-parameter model used for teaching and research). Also, consulting companies such as DasiSimulations (https://www.dasisim.com/) provide patients and physicians with an accurate patient-specific TAVR simulation and prediction of possible post-TAVR complications and outcomes. Even though there are sophisticated software and models already available for cardiovascular complications, software that can combine the TAVR biomechanics with hemodynamics to predict and optimize the exact outcomes of the TAVR during, shortly after, and in a long-term post-TAVR time span has not been developed.

Funding

Disclosure statement

Dr. Dasi and co-authors report patents filed on predictive computational modeling for planning structural heart procedures.

References

1   Leon MB, Mack MJ, Hahn RT, et al. Outcomes 2 years after transcatheter aortic valve replacement in patients at low surgical risk. *J Am Coll Cardiol.* 2021;77(9): 1149-1161.

2   Yanagisawa R, Hayashida K, Yamada Y, et al. Incidence, predictors, and mid-term outcomes of possible leaflet thrombosis after TAVR. *JACC Cardiovasc Imaging.* 2017; 10(1):1-11.

3   Pasic M, Unbehaun A, Buz S, Drews T, Hetzer R. Annular rupture during transcatheter aortic valve replacement: classification, pathophysiology, diagnostics, treatment approaches, and prevention. *JACC Cardiovasc Interv.* 2015;8(1 Part A): 1-9.

4   Bisson A, Bodin A, Herbert J, et al. Pacemaker implantation after balloon-or self-expandable transcatheter aortic valve replacement in patients with aortic stenosis. *J Am Heart Assoc.* 2020;9(9):e015896.

5   Ribeiro HB, Nombela-Franco L, Urena M, et al. Coronary obstruction following transcatheter aortic valve implantation: a systematic review. *JACC Cardiovasc Interv.* 2013;6(5):452-461.

6   Généreux P, Head SJ, Hahn R, et al. Paravalvular leak after transcatheter aortic valve replacement: the new Achilles' heel? A comprehensive review of the literature. *J Am Coll Cardiol.* 2013;61(11):1125-1136.

7   Wassef AWA, Rodes-Cabau J, Liu Y, et al. The learning curve and annual procedure volume standards for optimum outcomes of transcatheter aortic valve replacement: findings from an international registry. *JACC Cardiovasc Interv.* 2018;11(17): 1669-1679.

8   Sun W, Martin C, Pham T. Computational modeling of cardiac valve function and intervention. *Annu Rev Biomed Eng.* 2014;16:53-76.

9   Qin T, Caballero A, Mao W, et al. The role of stress concentration in calcified bicuspid aortic valve. *J R Soc Interf.* 2020;17(167):20190893.

10 Sun W, Abad A, Sacks MS. Simulated bioprosthetic heart valve deformation under quasi-static loading. *J Biomech Eng.* 2005;127(6):905-914.

11 Tzamtzis S, Viquerat J, Yap J, Mullen M, Burriesci G. Numerical analysis of the radial force produced by the Medtronic-CoreValve and Edwards-SAPIEN after transcatheter aortic valve implantation (TAVI). *Med Eng Phys.* 2013;35(1):125-130.

12 Bianchi M, Marom G, Ghosh RP, et al. Patient-specific simulation of transcatheter aortic valve replacement: impact of deployment options on paravalvular leakage. *Biomech Model Mechanobiol.* 2019;18(2):435-451.

13 Chen H, Yeats B, Swamy K, et al. Image registration-based method for reconstructing transcatheter heart valve geometry from patient-specific CT scans. *Ann Biomed Eng.* 2022. https://doi.org/10.1007/s10439-022-02962-9

14 Emendi M, Sturla F, Ghosh RP, et al. Patient-specific bicuspid aortic valve biomechanics: a magnetic resonance imaging integrated fluid–structure interaction approach. *Ann Biomed Eng.* 2021;49:627-641.

15 Lee JH, Rygg AD, Kolahdouz EM, et al. Fluid–structure interaction models of bioprosthetic heart valve dynamics in an experimental pulse duplicator. *Ann Biomed Eng.* 2020;48:1475-1490.

16 Luraghi G, Migliavacca F, García-González A, et al. On the modeling of patient-specific transcatheter aortic valve replacement: a fluid–structure interaction approach. *Cardiovasc Eng Technol.* 2019;10(3):437-455.

17 Buchanan RM, Sacks MS. Interlayer micromechanics of the aortic heart valve leaflet. *Biomech Model Mechanobiol.* 2014;13(4):813-826.

18 Zhang W, Rossini G, Kamensky D, Bui-Thanh T, Sacks MS. Isogeometric finite element-based simulation of the aortic heart valve: integration of neural network structural material model and structural tensor fiber architecture representations. *Int J Numer Method Biomed Eng.* 2021;37(4):e3438.

19 Bosmans B, Famaey N, Verhoelst E, Bosmans J, Vander Sloten J. A validated methodology for patient specific computational modeling of self-expandable transcatheter aortic valve implantation. *J Biomech.* 2016;49(13):2824-2830.

20 Finotello A, Morganti S, Auricchio F. Finite element analysis of TAVI: impact of native aortic root computational modeling strategies on simulation outcomes. *Med Eng Phys.* 2017;47:2-12.

21 Wang Q, Kodali S, Primiano C, Sun W. Simulations of transcatheter aortic valve implantation: implications for aortic root rupture. *Biomech Model Mechanobiol.* 2015; 14(1):29-38.

22 Dowling C, Bavo AM, El Faquir N, et al. Patient-specific computer simulation of transcatheter aortic valve replacement in bicuspid aortic valve morphology. *Circ Cardiovasc Imaging.* 2019;12(10):e009178.

23 Lavon K, Marom G, Bianchi M, et al. Biomechanical modeling of transcatheter aortic valve replacement in a stenotic bicuspid aortic valve: deployments and paravalvular leakage. *Med Biol Eng Comput.* 2019;57(10):2129-2143.

24 Singh-Gryzbon S, Ncho B, Sadri V, et al. Influence of patient-specific characteristics on transcatheter heart valve neo-sinus flow: an in silico study. *Ann Biomed Eng.* 2020;48:2400-2411.

25 El Faquir N, De Backer O, Bosmans J, et al. Patient-specific computer simulation in TAVR with the self-expanding Evolut R valve. *JACC Cardiovasc Interv.* 2020;13(15): 1803-1812.

26 Ueshima D, Fovino LN, Brener SJ, et al. Transcatheter aortic valve replacement for bicuspid aortic valve stenosis with first-and new-generation bioprostheses: a systematic review and meta-analysis. *Int J Cardiol.* 2020;298:76-82.

27 Yoon S-H, Kim W-K, Dhoble A, et al. Bicuspid aortic valve morphology and outcomes after transcatheter aortic valve replacement. *J Am Coll Cardiol.* 2020; 76(9):1018-1030.

28 Barbanti M, Yang TH, Rodès Cabau J, et al. Anatomical and procedural features associated with aortic root rupture during balloon-expandable transcatheter aortic valve replacement. *Circulation.* 2013;128(3):244-253.

29 Hansson NC, Nørgaard BL, Barbanti M, et al. The impact of calcium volume and distribution in aortic root injury related to balloon-expandable transcatheter aortic valve replacement. *J Cardiovasc Comput Tomogr.* 2015;9(5):382-392.

30 Willson AB, Webb JG, LaBounty TM, et al. 3-Dimensional aortic annular assessment by multidetector computed tomography predicts moderate or severe paravalvular regurgitation after transcatheter aortic valve replacement: a multicenter retrospective analysis. *J Am Coll Cardiol.* 2012;59(14):1287-1294.

31 Barbanti M, Leipsic J, Binder R, et al. Underexpansion and ad hoc post-dilation in selected patients undergoing balloon-expandable transcatheter aortic valve replacement. *J Am Coll Cardiol.* 2014;63(10):976-981.

32 Martin C, Sun W, Primiano C, McKay R, Elefteriades J. Age-dependent ascending aorta mechanics assessed through multiphase CT. *Ann Biomed Eng.* 2013;41: 2565-2574.

33 Aggarwal A, Ferrari G, Joyce E, et al. Architectural trends in the human normal and bicuspid aortic valve leaflet and its relevance to valve disease. *Ann Biomed Eng.* 2014;42(5):986-998.

34 Pasta S, Agnese V, Di Giuseppe M, et al. In vivo strain analysis of dilated ascending thoracic aorta by ECG-gated CT angiographic imaging. *Ann Biomed Eng.* 2017;45: 2911-2920.

35 Massing GK, James TN. Anatomical configuration of the His bundle and bundle branches in the human heart. *Circulation.* 1976;53(4):609-621.

36 Hamdan A, Nassar M, Schwammenthal E, et al. Short membranous septum length in bicuspid aortic valve stenosis increases the risk of conduction disturbances. *J Cardiovasc Comput Tomogr.* 2021;15(4):339-347.

37 Jilaihawi H, Zhao Z, Du R, et al. Minimizing permanent pacemaker following repositionable self-expanding transcatheter aortic valve replacement. *JACC Cardiovasc Interv.* 2019;12(18):1796-1807.

38 Chen Y-H, Chang H-H, Liao T-W, et al. Membranous septum length predicts conduction disturbances following transcatheter aortic valve replacement. *J Thorac Cardiovasc Surg.* 2020. https://doi.org/10.1016/j.jtcvs.2020.07.072

39 Rocatello G, Faquir NE, Santis GD, et al. Patient-specific computer simulation to elucidate the role of contact pressure in the development of new conduction abnormalities after catheter-based implantation of a self-expanding aortic valve. *Circ Cardiovasc Interv.* 2018;11(2):e005344.

40 Ribeiro HB, Webb JG, Makkar RR, et al. Predictive factors, management, and clinical outcomes of coronary obstruction following transcatheter aortic valve implantation: insights from a large multicenter registry. *J Am Coll Cardiol.* 2013; 62(17):1552-1562.

41 Ribeiro HB, Rodes-Cabau J, Blanke P, et al. Incidence, predictors, and clinical outcomes of coronary obstruction following transcatheter aortic valve replacement for degenerative bioprosthetic surgical valves: insights from the VIVID registry. *Eur Heart J.* 2018;39(8):687-695.

42 Jabbour RJ, Tanaka A, Finkelstein A, et al. Delayed coronary obstruction after transcatheter aortic valve replacement. *J Am Coll Cardiol.* 2018;71(14):1513-1524.

43 Yamamoto M, Shimura T, Kano S, et al. Impact of preparatory coronary protection in patients at high anatomical risk of acute coronary obstruction during transcatheter aortic valve implantation. *Int J Cardiol.* 2016;217:58-63.

44 Khan JM, Babaliaros VC, Greenbaum AB, et al. Preventing coronary obstruction during transcatheter aortic valve replacement: results from the multicenter international BASILICA registry. *JACC Cardiovasc Interv.* 2021;14(9):941-948.

45 Blanke P, Soon J, Dvir D, et al. Computed tomography assessment for transcatheter aortic valve in valve implantation: the Vancouver approach to predict anatomical risk for coronary obstruction and other considerations. *J Cardiovasc Comput Tomogr.* 2016;10(6):491-499.

46 Dvir D, Leipsic J, Blanke P, et al. Coronary obstruction in transcatheter aortic valve-in-valve implantation: preprocedural evaluation, device selection, protection, and treatment. *Circ Cardiovasc Interv.* 2015;8(1):e002079.

47 Mao W, Wang Q, Kodali S, Sun W. Numerical parametric study of paravalvular leak following a transcatheter aortic valve deployment into a patient-specific aortic root. *J Biomech Eng.* 2018;140(10):1010071-10100711.

48 Heitkemper M, Hatoum H, Azimian A, et al. Modeling risk of coronary obstruction during transcatheter aortic valve replacement. *J Thorac Cardiovasc Surg.* 2020; 159(3):829-838.e3.

49 Sivakumar SK, Yeats B, Polsani V, Yadav P, Thourani V, Dasi LP, editor. Computational modeling of coronary obstruction (CO) in Valve-in-Valve (ViV) Transcatheter Aortic Valve Replacement (TAVR): comparison with 2-dimensional CT based risk assessment. *Transcatheter Therapeutics (TCT) Meeting 2021; Orlando, FL*: 2021.

50 Chakravarty T, Søndergaard L, Friedman J, et al. Subclinical leaflet thrombosis in surgical and transcatheter bioprosthetic aortic valves: an observational study. *Lancet.* 2017;389(10087):2383-2392.

51 Makkar RR, Fontana G, Jilaihawi H, et al. Possible subclinical leaflet thrombosis in bioprosthetic aortic valves. *N Engl J Med.* 2015;373(21):2015-2024.

52 Rheude T, Pellegrini C, Stortecky S, et al. Meta-analysis of bioprosthetic valve thrombosis after transcatheter aortic valve implantation. *Am J Cardiol.* 2021;138: 92-99.

53 Szilveszter B, Oren D, Molnar L, et al. Subclinical leaflet thrombosis is associated with impaired reverse remodelling after transcatheter aortic valve implantation. *Eur Heart J Cardiovasc Imaging.* 2020;21(10):1144-1151.

54 Rashid HN, Nasis A, Gooley RP, Cameron JD, Brown AJ. The prevalence of computed tomography-defined leaflet thrombosis in intra- versus supra-annular transcatheter aortic valve prostheses. *Catheter Cardiovasc Interv*. 2018;92(7): 1414-1416.

55 Ruile P, Minners J, Breitbart P, et al. Medium-term follow-up of early leaflet thrombosis after transcatheter aortic valve replacement. *JACC Cardiovasc Interv*. 2018;11(12):1164-1171.

56 Franzone A, Pilgrim T, Haynes AG, et al. Transcatheter aortic valve thrombosis: incidence, clinical presentation and long-term outcomes. *Eur Heart J Cardiovasc Imaging*. 2018;19(4):398-404.

57 Hansson NC, Grove EL, Andersen HR, et al. Transcatheter aortic valve thrombosis: incidence, predisposing factors, and clinical implications. *J Am Coll Cardiol*. 2016; 68(19):2059-2069.

58 Casula M, Fortuni F, Ferlini M, et al. Subclinical leaflet thrombosis after transcatheter aortic valve replacement: a meaningless finding? A systematic review and meta-analysis. *Eur Heart J Qual Care Clin Outcomes*. 2021;7(1):107-108.

59 Jose J, Sulimov DS, El-Mawardy M, et al. Clinical bioprosthetic heart valve thrombosis after transcatheter aortic valve replacement: incidence, characteristics, and treatment outcomes. *JACC Cardiovasc Interv*. 2017;10(7):686-697.

60 Latib A, Naganuma T, Abdel-Wahab M, et al. Treatment and clinical outcomes of transcatheter heart valve thrombosis. *Circ Cardiovasc Interv*. 2015;8(4):e001779.

61 Rosseel L, De Backer O, Søndergaard L. Clinical valve thrombosis and subclinical leaflet thrombosis in transcatheter aortic heart valves: clinical manifestations, diagnosis, and treatment. *Precision Clin Med*. 2018;1(3):111-117.

62 Hafiz AM, Kalra A, Ramadan R, et al. Clinical or symptomatic leaflet thrombosis following transcatheter aortic valve replacement: insights from the U.S. FDA MAUDE database. *Struct Heart*. 2017;1(5-6):256-264.

63 Yanagisawa R, Tanaka M, Yashima F, et al. Early and late leaflet thrombosis after transcatheter aortic valve replacement. *Circ Cardiovasc Interv*. 2019;12(2): e007349.

64 Kakefuda Y, Hayashida K, Yamada Y, et al. Impact of subclinical vascular complications detected by systematic postprocedural multidetector computed tomography after transcatheter aortic valve implantation using balloon-expandable Edwards SAPIEN XT heart valve. *Am J Cardiol*. 2017;119(7):1100-1105.

65 Pache G, Schoechlin S, Blanke P, et al. Early hypo-attenuated leaflet thickening in balloon-expandable transcatheter aortic heart valves. *Eur Heart J*. 2016;37(28): 2263-2271.

66 Latib A, Testa L. Assessing the risk of leaflet motion abnormality following transcatheter aortic valve implantation. *Interv Cardiol Rev*. 2017;13(1):37-39.

67 De Backer O, Dangas GD, Jilaihawi H, et al. Reduced leaflet motion after transcatheter aortic-valve replacement. *N Engl J Med*. 2020;382(2):130-139.

68 Kanjanauthai S, Pirelli L, Nalluri N, Kliger CA. Subclinical leaflet thrombosis following transcatheter aortic valve replacement. *J Interv Cardiol*. 2018;31(5):640-647.

69 Oliveira DC, Okutucu S, Russo G, Martins ECC. The issue of subclinical leaflet thrombosis after transcatheter aortic valve implantation. *Cardiol Res*. 2020;11(5): 269-273.

70 Guedeney P, Mehran R, Collet JP, Claessen BE, Ten Berg J, Dangas GD. Antithrombotic therapy after transcatheter aortic valve replacement. *Circ Cardiovasc Interv*. 2019;12(1):e007411.

71 Rosseel L, De Backer O, Sondergaard L. Clinical valve thrombosis and subclinical leaflet thrombosis following transcatheter aortic valve replacement: is there a need for a patient-tailored antithrombotic therapy? *Front Cardiovasc Med*. 2019;6:44.

72 Rashid HN, Michail M, Ihdayhid AR, et al. Clinical predictors and sequelae of computed tomography defined leaflet thrombosis following transcatheter aortic valve replacement at medium-term follow-up. *Heart Vessels*. 2021;36:1374-1383.

73 Simpson TF, Tuohy CV, Rajotte K, et al. Bioprosthetic valve oversizing is associated with increased risk of valve thrombosis following TAVR. *Catheter Cardiovasc Interv*. 2021;97(3):E411-E417.

74 Khan JM, Rogers T, Waksman R, et al. Hemodynamics and subclinical leaflet thrombosis in low-risk patients undergoing transcatheter aortic valve replacement. *Circ Cardiovasc Imaging*. 2019;12(12):e009608.

75 Puri R, Auffret V, Rodes-Cabau J. Bioprosthetic valve thrombosis. *J Am Coll Cardiol*. 2017;69(17):2193-2211.

76 Sondergaard L, De Backer O, Kofoed KF, et al. Natural history of subclinical leaflet thrombosis affecting motion in bioprosthetic aortic valves. *Eur Heart J*. 2017;38(28): 2201-2207.

77 Vahidkhah K, Barakat M, Abbasi M, et al. Valve thrombosis following transcatheter aortic valve replacement: significance of blood stasis on the leaflets. *Eur J Cardiothorac Surg*. 2017;51(5):927-935.

78 Vahidkhah K, Azadani AN. Supra-annular Valve-in-Valve implantation reduces blood stasis on the transcatheter aortic valve leaflets. *J Biomech*. 2017;58:114-122.

79 Midha PA, Raghav V, Sharma R, et al. The fluid mechanics of transcatheter heart valve leaflet thrombosis in the neosinus. *Circulation*. 2017;136(17):1598-1609.

80 Khodaee F, Barakat M, Abbasi M, Dvir D, Azadani AN. Incomplete expansion of transcatheter aortic valves is associated with propensity for valve thrombosis. *Interact Cardiovasc Thorac Surg*. 2020;30(1):39-46.

81 Madukauwa-David ID, Sadri V, Kamioka N, et al. Transcatheter aortic valve deployment influences neo-sinus thrombosis risk: an in vitro flow study. *Catheter Cardiovasc Interv*. 2020;95(5):1009-1016.

82 Madukauwa-David ID, Sadri V, Midha PA, Babaliaros V, Aidun C, Yoganathan AP. An evaluation of the influence of coronary flow on transcatheter heart valve neo-sinus flow stasis. *Ann Biomed Eng*. 2020;48(1):169-180.

83 Plitman Mayo R, Yaakobovich H, Finkelstein A, Shadden SC, Marom G. Numerical models for assessing the risk of leaflet thrombosis post-transcatheter aortic valve-in-valve implantation. *R Soc Open Sci*. 2020;7(12):201838.

84 Wei ZA, Sonntag SJ, Toma M, Singh-Gryzbon S, Sun W. Computational fluid dynamics assessment associated with transcatheter heart valve prostheses: a position paper of the ISO Working Group. *Cardiovasc Eng Technol*. 2018;9(3):289-299.

85 Ghosh RP, Marom G, Bianchi M, D'Souza K, Zietak W, Bluestein D. Numerical evaluation of transcatheter aortic valve performance during heart beating and its post-deployment fluid-structure interaction analysis. *Biomech Model Mechanobiol*. 2020;19(5):1725-1740.

86 Hoda H, Shelly SS, Fateme E, et al. Correction to: predictive model for thrombus formation after transcatheter valve replacement. *Cardiovasc Eng Technol*. 2022. https://doi.org/10.1007/s13239-021-00601-3

87 Hoda H, Shelly S, Fateme E, et al. Predictive model for thrombus formation after transcatheter valve replacement. *Cardiovasc Eng Technol*. 2021;12:576-588.

88 Rahimtoola SH. The problem of valve prosthesis-patient mismatch. *Circulation*. 1978;58(1):20-24.

89 Pibarot P, Dumesnil JG. Hemodynamic and clinical impact of prosthesis-patient mismatch in the aortic valve position and its prevention. *J Am Coll Cardiol*. 2000; 36(4):1131-1141.

90 Stamou SC, Chen K, James TM, et al. Predictors and outcomes of patient-prosthesis mismatch after transcatheter aortic valve replacement. *J Card Surg*. 2020;35(2):360-366.

91 Ternacle J, Abbas AE, Pibarot P. Prosthesis-patient mismatch after transcatheter aortic valve replacement: has it become obsolete? *JACC Cardiovasc Interv*. 2021; 14(9):977-980.

92 Head SJ, Mokhles MM, Osnabrugge RL, et al. The impact of prosthesis-patient mismatch on long-term survival after aortic valve replacement: a systematic review and meta-analysis of 34 observational studies comprising 27 186 patients with 133 141 patient-years. *Eur Heart J*. 2012;33(12):1518-1529.

93 Kulik A, Al-Saigh M, Chan V, et al. Enlargement of the small aortic root during aortic valve replacement: is there a benefit? *Ann Thorac Surg*. 2008;85(1):94-100.

94 Pibarot P, Clavel MA. Prosthesis-patient mismatch after transcatheter aortic valve replacement: it is neither rare nor benign. *J Am Coll Cardiol*. 2018;72(22):2712-2716.

95 Pibarot P, Weissman NJ, Stewart WJ, et al. Incidence and sequelae of prosthesis-patient mismatch in transcatheter versus surgical valve replacement in high-risk patients with severe aortic stenosis: a PARTNER trial cohort–a analysis. *J Am Coll Cardiol*. 2014;64(13):1323-1334.

96 Dayan V, Vignolo G, Soca G, Paganini JJ, Brusich D, Pibarot P. Predictors and outcomes of prosthesis-patient mismatch after aortic valve replacement. *JACC Cardiovasc Imaging*. 2016;9(8):924-933.

97 Munoz-Garcia AJ, Munoz-Garcia M, Carrasco-Chinchilla F, et al. Incidence and clinical outcome of prosthesis-patient mismatch after transcatheter aortic valve implantation with the CoreValve prosthesis. *Int J Cardiol*. 2013;167(3):1074-1076.

98 Okuno T, Khan F, Asami M, et al. Prosthesis-patient mismatch following transcatheter aortic valve replacement with supra-annular and intra-annular prostheses. *JACC Cardiovasc Interv*. 2019;12(21):2173-2182.

99 Abbas AE. Prosthesis-patient mismatch following transcatheter aortic valve replacement: does size matter? *JACC Cardiovasc Interv*. 2020;13(1):138.

100 Abbas AE, Mando R, Hanzel G, et al. Invasive versus echocardiographic evaluation of transvalvular gradients immediately post-transcatheter aortic valve replacement. *Circ Cardiovasc Interv*. 2019;12(7):e007973.

101 Vlastra W, Chandrasekhar J, Munoz-Garcia AJ, et al. Comparison of balloon-expandable vs. self-expandable valves in patients undergoing transfemoral transcatheter aortic valve implantation: from the CENTER-collaboration. *Eur Heart J*. 2019;40(5):456-465.

102 Abdel-Wahab M, Mehilli J, Frerker C, et al. Comparison of balloon-expandable vs self-expandable valves in patients undergoing transcatheter aortic valve replacement: the CHOICE randomized clinical trial. *JAMA*. 2014;311(15):1503-1514.

103 Nombela-Franco L, Ruel M, Radhakrishnan S, et al. Comparison of hemodynamic performance of self-expandable CoreValve versus balloon-expandable Edwards SAPIEN aortic valves inserted by catheter for aortic stenosis. *Am J Cardiol*. 2013; 111(7):1026-1033.

104 Lerakis S, Hayek SS, Douglas PS. Paravalvular aortic leak after transcatheter aortic valve replacement: current knowledge. *Circulation*. 2013;127(3):397-407.

105 Kappetein AP, Head SJ, Genereux P, et al. Updated standardized endpoint definitions for transcatheter aortic valve implantation: the Valve Academic Research Consortium-2 consensus document (VARC-2). *Eur J Cardiothorac Surg*. 2012;42(5): S45-S60.

106 Généreux P, Piazza N, Alu MC, et al. Valve Academic Research Consortium 3: updated endpoint definitions for aortic valve clinical research. *Eur Heart J*. 2021; 42(19):1825-1857.

107 Giblett JP, Rana BS, Shapiro LM, Calvert PA. Percutaneous management of paravalvular leaks. *Nat Rev Cardiol*. 2019;16(5):275-285.

108 Yeats BB, Yadav PK, Dasi LP, et al. Treatment of Bicuspid Aortic Valve Stenosis with TAVR: Filling Knowledge Gaps Towards Reducing Complications. *Curr Cardiol Rep*. 2022:33-41.

109 Nappi F, Mazzocchi L, Spadaccio C, et al. CoreValve vs. Sapien 3 transcatheter aortic valve replacement: a finite element analysis study. *Bioengineering (Basel)*. 2021; 8(5):52.

110 Luraghi G, Matas JFR, Beretta M, Chiozzi N, Iannetti L, Migliavacca F. The impact of calcification patterns in transcatheter aortic valve performance: a fluid-structure interaction analysis. *Comput Methods Biomech Biomed Engin*. 2021;24(4):375-383.

111 Formaggia L, Quarteroni A, Veneziani A. *Cardiovascular Mathematics: Modeling and Simulation of the Circulatory System*. SpringerLink; 2009.

112 Auricchio F, Conti M, Lefieux A, et al. *Computational Methods in Cardiovascular Mechanics*. Taylor & Francis Group; 2018.

113 Pappalardo F, Russo G, Tshinanu FM, Viceconti M. In silico clinical trials: concepts and early adoptions. *Brief Bioinform*. 2019;20(5):1699-1708.
114 Restrepo M, Luffel M, Sebring J, et al. Surgical planning of the total cavopulmonary connection: robustness analysis. *Ann Biomed Eng*. 2015;43(6):1321-1334.
115 Fleeter CM, Geraci G, Schiavazzi DE, Kahn AM, Marsden AL. Multilevel and multifidelity uncertainty quantification for cardiovascular hemodynamics. *Comput Methods Appl Mech Eng*. 2020;365:113030.
116 Schiavazzi DE, Arbia G, Baker C, et al. Uncertainty quantification in virtual surgery hemodynamics predictions for single ventricle palliation. *Int J Numer Method Biomed Eng*. 2016;32(3):e02737.
117 Guzzetti S, Mansilla Alvarez LA, Blanco PJ, Carlberg KT, Veneziani A. Propagating uncertainties in large-scale hemodynamics models via network uncertainty quantification and reduced-order modeling. *Comput Methods Appl Mech Eng*. 2020; 358:112626.
118 Hughes TJR, Cottrell JA, Bazilevs Y. Isogeometric analysis: CAD, finite elements, NURBS, exact geometry and mesh refinement. *Comput Methods Appl Mech Eng*. 2005; 194(39):4135-4195.
119 Morganti S, Auricchio F, Benson DJ, et al. Patient-specific isogeometric structural analysis of aortic valve closure. *Comput Methods Appl Mech Eng*. 2015;284: 508-520.
120 Wu MCH, Muchowski HM, Johnson EL, Rajanna MR, Hsu M-C. Immersogeometric fluid–structure interaction modeling and simulation of transcatheter aortic valve replacement. *Comput Methods Appl Mech Eng*. 2019;357:112556.
121 Jan S. Hesthaven, Benjamin Stamm. *Certified Reduced Basis Methods for Parametrized Partial Differential Equations: Springer International Publishing*. 2016. volXIII:131p.
122 Quarteroni A, Manzoni A, Negri F. *Reduced Basis Methods for Partial Differential Equations: An Introduction*. SpringerLink; 2015:1-263.
123 Demo N, Tezzele M, Rozza G. EZyRB: easy reduced basis method. *J Open Source Softw*. 2018;3(24):661.
124 Liu M, Liang L, Sun W. Estimation of in vivo constitutive parameters of the aortic wall using a machine learning approach. *Comput Methods Appl Mech Eng*. 2019;347: 201-217.
125 Thériault-Lauzier P, Messika-Zeitoun D, Piazza N. Patient-specific computer simulation in TAVR. *JACC Cardiovasc Interv*. 2020;13(15):1813-1815.
126 Kandail HS, Trivedi SD, Shaikh AC, et al. Impact of annular and supra-annular CoreValve deployment locations on aortic and coronary artery hemodynamics. *J Mech Behav Biomed Mater*. 2018;86:131-142.
127 Kivi AR, Sedaghatizadeh N, Cazzolato BS, et al. Fluid structure interaction modelling of aortic valve stenosis: effects of valve calcification on coronary artery flow and aortic root hemodynamics. *Comput Methods Programs Biomed*. 2020;196:105647.
128 Shahrul HM, Mitsugu T. Fluid-structure interaction simulation of artificial heart valve considering open state of cardiac cycle. *J Biotechnol Biomed*. 2021;4:124-131.
129 Cai L, Zhang R, Li Y, et al. The comparison of different constitutive laws and fiber architectures for the aortic valve on fluid–structure interaction simulation. *Front Physiol*. 2021;12(725):682893.
130 Lan H, Updegrove A, Wilson NM, Maher GD, Shadden SC, Marsden AL. A re-engineered software interface and workflow for the open-source SimVascular cardiovascular modeling package. *J Biomech Eng*. 2018;140(2):0245011-02450111.
131 Updegrove A, Wilson NM, Merkow J, Lan H, Marsden AL, Shadden SC. SimVascular: an open source pipeline for cardiovascular simulation. *Ann Biomed Eng*. 2017;45(3):525-541.
132 Arthurs CJ, Khlebnikov R, Melville A, et al. CRIMSON: an open-source software framework for cardiovascular integrated modelling and simulation. *PLoS Comput Biol*. 2021;17(5):e1008881.
133 *WinNonlin® Version 6.4 (Certara USA, Inc)*. 2014.
134 Plank G, Loewe A, Neic A, et al. The openCARP simulation environment for cardiac electrophysiology. *bioRxiv*. 2021. https://doi.org/10.1101/2021.03.01.433036
135 Heldt T, Mukkamala R, Moody GB, Mark RG. CVSim: an open-source cardiovascular simulator for teaching and research. *Open Pacing Electrophysiol Ther J*. 2010;3:45-54.